Prodigiosin-functionalized *Lactobacillus acidophilus ghost*: A bioinspired combination against colorectal cancer cells

Nessrin Saleh
Alexandria University
Hoda Mahmoud (hoda_eltalkhawy@alexu.edu.eg)
Alexandria University
Hoda Eltaher
Alexandria University
Maged Helmy
Damanhour University
Labiba El-Khordagui (labiba.elkhordagui@alexu.edu.eg)
Alexandria University
Ahmed Hussein (ahmed.hussien@alexu.edu.eg)
Alexandria University

Research Article

Keywords: Lactobacillus acidophilus ghosts, drug delivery system, colorectal cancer, prodigiosin

Posted Date: March 23rd, 2021

DOI: https://doi.org/10.21203/rs.3.rs-350303/v1

Abstract

Lactobacillus acidophilus ghosts (LAGs) with the unique safety of a probiotic, inherent tropism for colon cells and multiple bioactivities offer great promise as drug carrier for colon targeting. We report herein on a novel bioinspired drug delivery system against colorectal cancer (CRC) cells based on LAGs functionalized with prodigiosin (PG), a proapoptotic bacterial metabolite. LAGs were prepared by a chemical method and highly purified by density gradient centrifugation. Multiple microscopic and staining techniques characterized LAGs by a relatively small size, size uniformity, a relatively large internal volume devoid of cytoplasmic and genetic materials and an intact negatively charged envelop. PG was highly bound to LAGs cell wall, generating a physiologically stable bioactive entity (PG-LAGs) active against HCT116 CRC cells at the cellular and molecular levels. Cell viability data underlined cytotoxicity of PG and LAGs and LAGs-induced enhancement of PG selectivity for HCT116 cells. Combination and Dose reduction indices anticipating dose reduction of PG and LAGs. Molecularly, PG-LAGs significantly modulated the expression of apoptosis-related biomarkers, caspase 3, P53 and BCL2, in favor of cytotoxicity against HCT116 cells relative to PG and 5-fluorouracil. Accordingly, LAGs offer promise as novel drug carrier for targeted colon delivery and PG-LAGs may bring therapeutic benefits in colorectal carcinoma.

Introduction

Bacterial cells have attracted growing attention as a sustainable source of bacterial-derived structures and byproducts of great benefit in biomedical applications [1–3]. Amongst bacterial-derived structures, bacterial ghosts (BGs) represent an advancing biotechnological platform in the prevention and treatment of disease. BGs are intact envelopes of bacterial cells, emptied of their cytoplasmic and genetic materials by gentle poring methods. While the genetic method has been commonly utilized for the preparation of Gram negative bacterial ghosts [4], chemical methods allowed the generation of BGs of both Gram negative and Gram positive bacteria [5,6].

BGs retain the cellular morphology and surface structural components of native cells, most importantly antigenic proteins to be recognized by the immune system as well as fimbriae and adhesins to facilitate targeting and binding to different cells and tissues [7,8]. Such outstanding surface features endow BGs with the ability to stimulate immune responses, provide natural adjuvant properties and serve as vector in the delivery of human and veterinary vaccines [9]. Equally important, BGs are emerging as a multifunctional platform in drug and gene therapy. In this regard, BGs may have therapeutic potentials on their own and may synergize the activity of other drugs via BG-induced immunostimulatory effects [10]. BGs show several intrinsic merits as drug carriers compared with biomaterial-based delivery systems. These include primarily stability in the biological milieu, large internal space, greater safety allowing for larger doses in addition to inherent tropism-targeted drug delivery [2,11]. Promising effects have been achieved recently with BG-mediated targeted delivery of anticancer drugs [12,13] and macrophage delivery of anti-infective agents [14].

However, bacteria used for the preparation of BGs to date are mostly pathogenic and the utilization of non-pathogenic bacteria would greatly enhance the safety profile of BG-based drug delivery systems. To this end, Gram positive lactic acid probiotic bacteria with significant health-promoting effects, are generally recognized as safe (GRAS) and have demonstrated immunomodulatory capability [15]. Moreover, several anticancer effects have been associated with their structural components and metabolites [16,17]. Among the best known lactic acid bacteria, *Lactobacillus acidophilus* (LA) naturally colonize the human colon with resilient adhesive properties as a result of binding to mucin [18] and recognition of their antigens by colon cells and the adjacent immune system [19].

Such distinct properties render LA ghosts (LAGs) highly promising drug carriers for targeting colorectal cancer (CRC) cells. To date, drug delivery by BGs has been generally restricted to chemotherapeutic agents such as 5-fluorouracil [13] and doxorubicin [20]. Nevertheless, functionalizing BGs with bacterial metabolites having colorectal cancer inhibitory activity may establish a new microbially-derived biotherapeutic platform for the treatment of CRC, one of the most common malignancies worldwide. In this regard, prodigiosin (PD), a secondary metabolite of *Serratia marcescens* (*S. marcescens*), induces significant cytotoxic effects in diverse cancer cell lines [21] without induction of marked toxicity in nonmalignant cell lines [22]. PG's selective anti-colorectal actions are believed to occur via apoptosis as a result of alteration of the expression of apoptosis-related genes [23,24] and restoration of p53 tumor suppressor activity in chemoresistant CRC stem cells [25]. PG was also shown to reduce survivin levels and increase caspase-3 and miRNA-16-1 levels in CRC stem-like cells [22,24]. Besides, PG sensitizes CRC cells to cell death induced by anti-cancer drugs [22,26].

The objective of the present study was to develop PG-functionalized LAGs (PG-LAGs) as a novel microbially inspired anti-cancer drug delivery system integrating the aforementioned potentials of PG and LAGs for targeting CRC cells. The study involves preparation, purification, and characterization of blank LAGs as well evaluation of LAGs as drug carrier in terms of size, size uniformity, PG loading capacity, and release properties. Finally, the activity of PG-LAGs against CRC cells in comparison with PG, LAGs, and 5-fluorouracil as standard treatment was assessed at the cellular level using HCT116 CRC cell line and molecularly by determining the level of three apoptosis-related biomarkers, caspase 3, P53 and BCL 2 in CHT116 cellular proteins.

Results

Preparation and differentiation of Lactobacillus acidophilus ghosts (LAGs). The chemical SLRP used for the preparation of LAGs using NaOH and SDS as described in the methods section generated a bacterial mass consisting of a mixture of bacterial LAGs, dead un-evacuated LA cells and the remaining live LA cells which tolerated chemical lysis. Differentiation of LAGs from LA cells in the bacterial mass was achieved using a new light microscopic method based on toluidine blue, a dye known to bind to DNA. Figure 1 indicated that live LA cells acquired the intense toluidine blue color (Fig. 1a) while the presence of LAGs [illegible] obvious reduction in the blue staining of the

bacterial mass (Fig. 1b). Moreover, comparison of intracellular content by TEM imaging of live LA cells (Fig. 1c) and the bacterial mass (Fig. 1d) verified the presence of a mixture of evacuated LAGs and un-evacuated LA cells in the mass. Attempts to increase the yield of LAGs in the bacterial mass by increasing the concentration of NaOH and SDS or applying the chemical treatment under static conditions resulted in rupture of the ghost cell wall (Fig. 1e and f).

Purification of L. acidophilus ghosts (LAGs) by density gradient centrifugation. Subjecting a suspension of the bacterial mass in saline to a two-step density gradient centrifugation resulted in effective separation of light-weight LAGs as a high purity fraction. The first centrifugation steps at 168 xg for different time intervals (6, 9, 12, 15, 18 min) were effective in eliminating the heavy dead un-evacuated LA cells as well as the remaining live cells. The final centrifugation step (20 min at 672 xg) precipitated the lighter bacterial ghosts. As shown in Fig. 2, light microscopy indicated absence of toluidine blue-stained LA cells (Fig. 2a) which was verified by TEM (Fig. 2b) and the absence of growth upon inoculating a MRS plate with the purified LAGs for 48 h at 37°C (Fig. 2c).

Characterization of purified L. acidophilus ghosts (LAGs). Purified LAGs were characterized for morphology and intracellular content by SEM and TEM respectively (Fig. 3Aa-f), expulsion of genetic materials and intracellular cytoplasm and cell wall proteins by gel electrophoresis (Fig. 3Ba and b), in addition to integrity of the ghost capsule (Fig. 3Ca) and preservation of the cell wall surface negative charge (Fig. 3Cb) using staining methods.

LAG morphology and intracellular content. As indicated by SEM at 35000x of live LA cells (Fig. 3Aa) and LAGs (Fig. 3Ab), the surface structures of LAGs appeared intact similar to those of live cells except for the existence of pores from which the intracellular contents were expelled. TEM imaging (Fig. 3Ac-f) indicated that compared with live LA cells (Fig. 3Ac), LAGs appeared empty with retention of a cohesive cell wall (Fig. 3Ad-f). The calculated internal volume of LAGs was 0.13 μm^3 approximately and the pores with a mean size of 153.63 ± 12.23 nm were located at the division sites representing the weak point of the bacterial wall (Fig. 3Ae, f).

Elimination of genetic materials and proteins. Elimination of genetic materials was confirmed by agarose gel electrophoresis of DNA following DNA extraction from LAGs and live LA cells. As revealed by Fig. 3Ba, LAGs were devoid of nucleic acids. Expulsion of the total protein content of live LA and proteins of LA envelops were verified by SDS-PAGE electrophoresis (Fig. 3Bb). The total protein content of live LA cells (Lane 1) was larger than that of LAGs (Lane 2), confirming evacuation of LAGs from cytoplasmic materials. In addition, Lane 3 for the protein profiles of the supernatant after chemical treatment revealed expulsion of the LAGs proteins into the supernatant.

Integrity and negativity of the L. acidophilus ghosts. The integrity and surface negativity of LAGs envelop were demonstrated by light microscopic imaging of LAGs in comparison with live LA cells using crystal violet/copper sulphate (Antony's stain) and nigrosine staining, respectively (Fig. 3C). Antony's staining revealed existence of an intact capsule in both live bacteria (Fig. 3Ca) and LAGs (Fig. 3Cb). Insets in both

figures showed a faint copper sulphate blue halo (capsule) around crystal violet-stained purple cells indicating integrity of the capsule. Nigrosine staining affirmed that the negativity of the cell wall of live LA cells (Fig. 3Cd) was preserved in LAGs (Fig. 3Cd) after chemical treatment, both appearing as bright halos on the dark background.

Prodigiosin-functionalized *L. acidophilus* ghosts

Preparation. Loading of PG via incubating blank LAGs with PG solution in a methanol: acetic acid solvent system was affected by the solvent composition, PG concentration, incubation time and agitation rate. In a series of single point experiments, the highest PG loading efficiency achieved by incubating LAGs with a 2 mg/mL PG in a methanol: acetic acid (1:1) for 2 h with agitation at 200 rpm was 3.9 %.

Physical Characterization. The size of blank LAGs determined by dynamic light scattering was 1.13 ± 0.13 μm with a PDI 0.15 ± 0.09 while that of PG-LAGs was 1.59 ± 0.24 μm with PDI 0.27 ± 0.04. ZP measurements revealed a relatively low negative surface charge for blank LAGs (-4.20 ± 4.22 mV) and PG-LAGs (-0.821 ± 4.03 mV).

Verification of PG entrapment in LAGs. PG entrapment in LAGs was verified by digital photography, light microscopy, and TEM (Fig. 4a-h). Compared with blank LAGs, the pellet of PG-LAGs acquired the characteristic red color of PG as indicated by digital photos (Fig. 4a and e). PG-LAGs also appeared as red vesicles under the 100x lens of the light microscope without staining (Fig. 4b and f). TEM imaging at 20000x revealed that the density of the cell wall of blank LAGs (Fig. 4c) was obviously increased in PG-LAGs (Fig. 4g), with maintenance of the calculated internal volume (≈ 0.13 μm^3) unchanged. TEM also demonstrated binding of PG to the LAG cell wall with no evident damaging effects as affirmed by images of LAGs and PG-LAGs at 80000x (Fig. 4d and h respectively).

Release studies. Data for PG release from PG-LAGs at 37°C in media of different pH (acetate buffer pH 5.5 and phosphate buffer saline pH 7.4 with or without the addition of 5% methanol) at 100 rpm for 24 h indicated high PG retention by LAGs which could not be overcome by the inclusion of up to 3% Tween 80. Similar results were obtained for the release of PG in simulated gastric and simulated intestinal fluids. Moreover, PG was almost completely recovered from PG-LAGs at the end of the release experiments by extraction with methanol.

Cytotoxicity studies

Cell viability, IC50 and selectivity index (SI). Cytotoxicity data expressed as % viability of HCT116 CRC cells upon exposure to the test preparations at increasing concentrations for 24 h at 37°C using MTT assay are shown in Fig. 5a-d. Cell viability curves for 5-fluorouracil (5-FU) (Fig. 5a), PG (Fig. 5b), LAGs (Fig. 5c) and PG-LAGs (Fig. 5d) showed a concentration-dependent effect within their respective concentration ranges.

The IC50 values computed from cell viability data (Table 1) indicated that the IC50 of PG (2.026 ± 0.17 µg/mL) was slightly higher than that of 5-FU (1.483 ± 0.19 µg/mL) with a non-statistically significant difference ($p > 0.05$). Moreover, a combination of PG and LAGs in PG-LAGs induced ≈ 8.5-fold reduction in the IC50 of LAGs. The selectivity of the test preparations for HCT116 CRC expressed as the selectivity index (SI) (IC50 values in normal human fibroblasts relative to those in HCT 116 cells) indicated significantly greater ($p < 0.05$) selectivity of PG (17.87), LAGs (28.24) and PG-LAGs (43.60) for HCT116 cells relative to 5-FU (8.63). Furthermore, the SI index of PG and LAGs was significantly increased ($p < 0.05$) by their combination in PG-LAGs.

Table 1
IC50 values for 5-fluorouracil (5-FU), prodigiosin (PG), *L. acidophilus* ghosts (LAGs) and PG-functionalized LAGs (PG-LAGs) in HCT116 colorectal cancer cells and normal human fibroblasts and the derived selectivity index (SI).

Preparations	IC50 in HCT-116 cell line (µg/mL)	IC50 in normal fibroblasts (µg/mL)	Selectivity index (SI)
5-FU	1.48 ± 0.19	12.77 ± 1.04	8.63
PG	2.03 ± 0.17	36.28 ± 6.91	17.87
LAGs	393.44 ± 4.20	11110.0 ± 59.21	28.24
PG:BG (1:25)	46. 47 ± 1.74	2027.37 ± 92.15	43.60

Combination index (CI) and dose reduction index (DRI). Values for the Combination Index (CI) and Dose Reduction Index (DRI) are shown in Table 2. CI is a parameter used to indicate synergistic (CI < 1), additive (CI = 1) or antagonistic (CI > 1) effects of 2 drugs in combination while the Dose Reduction Index (DRI) expresses the synergy of two drugs and indicate the fold-decrease in the dose of each drug independently related to their dose in the combination. Both CI and DRI values were generated by analysis of the combinatorial cytotoxic effect of PG-LAGs on HCT116 cells following 24 h treatment at EC50 (Effective dose for 50% cell viability inhibition achieved by the combination). The CI was 0.997, indicating a synergistic cytotoxic effect of PG and LAGs. The concentrations of PG and LAGs as single components at EC50 were 2.026 µg/mL and 393.440 µg/mL, respectively. These were reduced by combining both agents in PG-LAGs to 1.79 µg/mL and 44.68 µg/mL respectively, producing DRI values > 1 with 1.13 - and 8.81-fold dose reduction for PG and LAGs, respectively.

Table 2
Combination Index (CI) and Dose Reduction Index (DRI) generated by CompuSyn analysis of the combined cytotoxic effects of prodigiosin (PG) and *L. acidophilus* ghosts (LAGs) either singly or combined as PG-LAGs (1:25) on HCT116 CRC cell line for 24 h at EC50 (Effective dose for 50% cell viability inhibition by the combination). PG concentration range 0.25-10 µg/mL.

EC	Combination Index (CI)	Concentration of PG and LAGs as single agents		Concentration of PG and LAGs combined in PG-LAGs		Dose Reduction Index (DRI)	
		PG (µg/mL)	LAGs (µg/mL)	PG (µg/mL)	LAGs (µg/mL)	PG	LAGs
50	0.997	2.026	393.440	1.79	44.68	1.13	8.81

Effect of test preparations on apoptosis-related biomarkers. The effect of PG, LAGs, and PG-LAGs in comparison with 5-FU on the level of three apoptosis-related biomarkers, namely caspase-3, P53 and BCL 2 per mg of HCT116 cellular protein is illustrated in Fig. 6a-c.

Caspase 3 activity. Figure 6a indicated a significant increase ($p < 0.05$) in the activity of the apoptotic caspase 3 by all treatments relative to control. The difference between single treatments was not statistically significant. However, PG-LAGs exerted a significantly greater ($p < 0.05$) increase in caspase 3 activity relative to its single PG and LAGs components and 5-FU.

p53 protein level. As shown in Fig. 6b, expression of the pro-apoptotic P53 protein was significantly increased ($p < 0.05$) by all treatments, though the greatest upregulating effect was exerted by PG-LAGs. The PG-LAGs effect was significantly greater ($p < 0.05$) than that of its single components but not 5-FU.

BCL 2 protein level. The level of the anti-apoptotic cellular BCL 2 protein (Fig. 6c) was significantly ($P < 0.05$) reduced by all treatments. However, reduction by PG-LAGs was significantly greater ($P < 0.05$) than that exerted by its single components but not 5-FU.

Discussion

LAGs were prepared, purified, and characterized for application as novel drug carriers for colon targeting. The chemical SLRP method [27] with modification involving replacement of H_2O_2 and $CaCO_3$ with NaOH and SDS at their respective MGC and MIC generated a bacterial mass containing LAGs in addition to un-evacuated dead LA cells and live LA cells which resisted chemical lysis. Differentiation of LAGs from other cells could be achieved utilizing a new simple and economic method based on toluidine blue, a basic thiazine molecule known to highly bind to nucleic acids [28]. The differentiative ability of the toluidine staining method was verified by light microscopy and TEM (Fig. 1a-d), which indicated incomplete lysis of LA cells. Attempts to increase the proportion of LAGs in the mass by increasing NaOH and SDS concentrations or exposing LAGs to harsher conditions resulted in cell wall rupturing (Fig. 1e

and f). As such, the product of chemical lysis was a bacterial mass consisting of LAGs in combination with live and dead un-evacuated LC cells.

A purified fraction of LAGs could be separated from the bacterial mass by density gradient centrifugation [29], a method not documented to date for the separation of ghosts from un-evacuated bacterial cells. Microscopical and microbiological verification of the purity of the separated ghost fraction (Fig. 2) ascertained the efficiency of the density gradient centrifugation as a practical method for the separation of ghosts from a bacterial mass. Characterization of the purified LAGs by SEM and TEM, gel electrophoresis and light microscopy (Figs. 3A-C) collectively verified the morphology of LAGs as empty vesicles devoid of cytoplasmic content with an internal volume of 0.13 μm^3 approximately and surrounded by an intact and cohesive negatively charged cell wall having pores with a mean size of 153.63 ± 12.23 nm located at the division sites representing the weak point of the bacterial cell wall. Agarose gel electrophoresis and SDS-PAGE confirmed elimination of genetic materials and intracellular proteins respectively from LAGs with preservation of their membrane proteins. Retention of an intact capsule around LAGs following chemical treatment is a crucial factor in their adhesion to cellular membranes, a process mediated by the capsular polysaccharides cohesive layer [30]. Moreover, the surface negativity of LAGs denoted retention of lipoteichoic acid, a strongly negatively charged surface-associated element that contributes to the integrity of the membrane of LA cells [31] and their adhesion to colon cells [32,33]. This implied maintenance of targeting ability of the live cells by the ghost.

Findings obtained so far suggested benefits of purified LAGs as a drug carrier characterized by an intracellular space of 0.13 μm^3 approximately and a negatively charged intact membrane as potential sites for drug loading in addition to surface characteristics favoring inherent tropism for colon cells. Applicability of LAGs in drug delivery was supported by favorable pharmaceutical attributes including a relatively small size (1.13 ± 0.13 µm) and size distribution (PDI 0.15 ± 0.09). Promotion of LAGs as bio-inspired anti-CRC delivery system was achieved by the incorporation of PG, a secondary bacterial metabolite with established apoptotic activity against CRC. However, the development of PG-functionalized LAGs was challenged by the high hydrophobicity of PG (log $P_{\text{octanol–water}}$ 5.16) and its poor solubility in aqueous physiological media, a well-documented PG formulation problem [34–36]. A simple incubation method allowed 3.9% loading of LAGs by varying the composition of a methanol-acetic acid solvent system, temperature, incubation time and agitation rate. The solvent system had a key role in PG loading as it was shown to promote permeabilization of the bacterial phospholipid bilayer [37,38] and protonation of PG [39,40]. This would enhance PG binding to the negatively charged LAG membrane via strong electrostatic interaction PG loading which was confirmed by digital and microscopic imaging (Fig. 4a-h).

In vitro release data obtained in buffers with different pH and simulated gastrointestinal fluids at 100 rpm and 37°C indicated retention of PG by LAGs for the 24 h-study period. Complete recovery of the amount of PG loaded into LAGs by extraction with methanol at the end of the release experiments suggested high stability of the PG-LAG system in physiological media. Drug release properties of bacterial ghosts

(BGs) may differ greatly from those of polymer-based drug carriers which usually undergo marked physicochemical changes under the release conditions contributing to drug liberation. For instance, sustained release of PG from PLGA microparticles in PBS pH 7.4 containing 0.1% w/v Tween 80 at 37°C was mediated by a combination of diffusion-, dissolution- and polymer degradation-controlled mechanisms [36]. Similarly, release of PG from chitosan microspheres at pH 7.4 involved porosity and degradation of the polymer matrix [41]. Strong binding of PG to LAGs, as a result of localization of PG molecules within the resistant ghost capsule and electrostatic interaction with the negatively charged cell wall components in addition to structural stability of LAGs, appear to preclude PG release. PG and other hydrophobic bioactive agents were reported to interact with lipophilic components of the cell membranes of bacterial cells and ghosts [35,42]. In fact, drug release from BGs depends mainly on the type of ghost and the drug physicochemical properties. While *E. coli* ghosts failed to release resveratrol [42], 12% of doxorubicin was released from *Mannheimia haemolytica* ghosts in 10 h [43]. Accordingly, release data implied strong PG binding to LAGs, probably constituting a single bioactive entity.

Despite lack of PG release from LAGs, activity of PG-LAGs against HCT116 CRC cells demonstrated at both the cellular and molecular levels indicated that PG payload (40 µg/mg) was sufficiently bioactive, providing a proof of concept for potential application of PG-LAGs as an anti-CRC bacterial structure. It is worth noting that trafficking and targeting of drugs by bacterial structures may involve mechanisms which do not necessarily depend on extracellular drug delivery [2]. These include fusion of the bacterial structure with cell membranes of the target cells with subsequent release of their cargo inside the cytoplasmic space as reported for doxorubicin loaded ghosts [43] or cellular uptake followed by release of the drug after endosomal escape [42,44]. Uptake of bacterial ghosts by different cells such as antigen presenting cells [45] and conjunctival epithelial cells [46] has been reported.

Indeed, cell viability data obtained following 24 h treatment of HCT116 cells, a model for CRC initiating cells with stem-like cells properties [24] generated multiple important findings. These include a PG cytotoxic effect approaching that of 5-FU, the first-line treatment for colorectal cancer (CRC), with insignificantly different IC50 values. Such a considerable PG cell viability suppressing effect can be explained by the well-established activity of PG against cancer CRC cells [34] in addition to its apoptotic activity against cancer stem cells [24,25] which account for a relatively large proportion of HCT116 cells [47]. In contrast, 5-FU does not inhibit CRC stem cells [48]. Interestingly, blank LAGs exerted a cytotoxic effect against HCT116 cells, corroborating data *for E. coli* ghosts against Caco-2 cell line [13]. This is a valuable merit of LAGs as bioactive carrier for colon targeting knowing that some bacterial ghosts might exert a cancer cell proliferating effect [43]. The cytotoxic activity of LAGs was significantly enhanced by PG loading, achieving ≈ 8.5-fold reduction in LAGs IC50 as well as an increase in their selectivity for HCT116 cancer cells, surpassing 5-FU selectivity (Table 1). The notable safety of LAGs to normal human fibroblasts cells, their inherent tropism for colon cells and possible cellular uptake may account for the relatively high selectivity of PG-LAGs for CRC cells. Importantly, analysis of the combinatorial anticancer effects of PG and LAGs in PG-LAGs following a relatively short 24 h incubation with HCT116 cells pointed to synergism

that was associated with an anticipated 1.13- fold and 8.81-fold reduction in the dose of PG and LAGs respectively in the combination at EC50 (Table 2).

Anti-cancer merits of PG-LAGs demonstrated at the cellular level were substantiated at the molecular level by significant modulation of the levels of apoptosis-related biomarkers in HCT116 intracellular protein (Fig. 6a-c). PG and LAGs in comparison with 5-FU showed a significant increase in the intracellular apoptotic caspase 3 activity and P53 protein level and significant downregulation of the anti-apoptosis-related B-cell lymphoma 2 (BCL 2) protein level relative to untreated control cells. LAGs-induced molecular effects supported the intrinsic tropism and cytotoxicity of LAGs against CRC cells, an issue warranting further investigation. Upregulation of caspase 3 activity and apoptosis of HCT116 by PG was shown previously to depend on a decrease in the mRNA and protein levels of the proto-oncogene survivin [24]. Induction of caspase-3 activation through the survivin inhibition pathway in both HTC116 and HT-29 CRC cells [23,24] may provide a molecular mechanism for PG-induced apoptosis.

PG and LAGs as well as 5-FU also upregulated P53, a tumor suppressor frequently mutated or inactivated in colorectal cancer. The individual effects of PG and LAGs were significantly exceeded by that of PG-LAGs. PG was shown to restore the p53 pathway known to target CRC stem cells representing a considerable proportion of HCT116 cells via activation of p73, a member of the p53 family [25], leading to cell growth inhibition. BCL 2 which belongs to the BCL 2 protein family plays an essential role in the intrinsic mitochondrial apoptotic signaling pathway. Thus, the anti-apoptotic BCL 2 protein may support cell survival and induce drug resistance in cancer cells [49]. The level of BCL2 protein in the untreated control HCT116 cells was significantly reduced by all test preparations, though reduction by PG-LAGs was significantly greater than that of PG and LAGs but not 5-FU. Activation of caspase 3 combined with upregulation of P53 and downregulation of BCL 2 demonstrated high pro-apoptotic capacity of PG-LAGs in the treated HCT116 cells. The significantly greater modulating effect of PG-LAGs relative to PG and LAGs can be explained by enhanced intracellular activities as a result of fusion or uptake of PG-LAGs by the HCT116 CRC cells. Results highlighted activity of LAGs against CRC cells, promoting their utilization as a novel bacterial ghost species carrier for colon targeting in addition to the potentials of PG-LAGs in the treatment of colorectal carcinoma.

Conclusions

A novel bio-inspired prodigiosin-functionalized *L. acidophilus* ghosts (PG-LAGs) for colon targeting that combines the safety, bioactivity, and inherent affinity of a probiotic LAGs for colon cells and the apoptotic activity of PG against CRC was developed. The study provides new methodological information on the generation of high-quality ghosts of the Gram-positive LA and their effective purification using a density gradient centrifugation technique not documented to date. Moreover, toluidine blue binding to DNA proved effective as a new simple and economic staining method for the differentiation of ghosts from un-evacuated bacterial cells. Loading of PG into bacterial ghosts generated a novel microbially derived bioactive structure with high membrane integrity and stability under physiological conditions. Despite

ivity against CRC HCT116 cells at the cellular

and molecular levels suggested cellular fusion or uptake of PG-LAGs. Significantly enhanced selectivity and apoptotic activity of PG by entrapment in LAGs strongly suggest LAGs as novel probiotic drug carrier for targeted colon delivery and PG-LAGs as a microbially derived potential biotherapeutic for colorectal carcinoma.

Materials And Methods

Preparation and differentiation of Lactobacillus acidophilus **ghosts (LAGs).** *L. acidophilus* (LA) ATCC 4356 was obtained from WFCC-MIRCEN-World Data Centre for Microorganisms (http://www.wdcm.org/), Faculty of Agriculture, Ain Shams University, Cairo, Egypt. De Man, Rogosa and Sharpe (MRS) broth and agar were used for growing and preservation of LA (HiMedia Laboratories, India). LAGs were prepared using essentially the chemical sponge-like reduced protocol (SLRP) [27] with some modification. Briefly, MRS broth was inoculated with a single colony of overnight LA culture and incubated at 37°C for 72 h. Bacterial cells were harvested by centrifugation at 672 xg for 10 min and pellets were washed twice with 0.5% NaCl. Washed LA cells were incubated in a mixture NaOH at the minimum growth concentration (MGC, 0.01%) and sodium dodecyl sulphate at the minimum inhibitory concentration (MIC, 0.1%) with shaking at 120 rpm overnight (16–18 h) at 37°C. Bacterial pellets were harvested by centrifugation at 672 xg for 10 min and washed twice with 0.5% NaCl solution. The bacterial mass obtained presumably consisted of a combination of LAGs and live and dead un-evacuated LA cells. Differentiation of LAGs from un-evacuated LA cells was achieved by toluidine blue staining and TEM. For toluidine staining, a bacterial suspension and ghost suspension were smeared on the surface of a glass slide and fixed by gentle heating. The slides were stained with toluidine blue dye (0.1%) for 15 min, washed with a few drops of water, air-dried, and examined under the oil immersion lens of a light microscope (Olympus CX31 Microscope). Live LA cells and LAGs were examined by transmission electron microscopy (TEM, JEOL-JSM-1400 PLUS) as reported [50].

Purification of L. acidophilus **ghosts (LAGs) by density gradient centrifugation.** LAGs were purified by separation from live and dead un-evacuated LA cells by subjecting the resuspended bacterial mass to a density gradient centrifugation technique [29] for different time intervals (6, 9, 12, 15, 18 min) at 168 x g. This was followed by centrifugation of each separated fraction for 20 min at 672 xg to precipitate LAGs. To assess the efficiency of the separation procedure, the purified LAGs obtained at the end of the centrifugation process were examined by light microscopy following toluidine blue staining, TEM imaging and culture on MRS agar plates at 37°C for 48 h.

Characterization of L. acidophilus **ghosts.** LAGs were examined in comparison with live LA cells for morphology, elimination of cytoplasmic and genetic materials, in addition to integrity and negativity of the cell wall. The morphology and intracellular content of LAGs in comparison with live LA cells were examined by scanning electron microscopy (SEM, JSM-5300 (JEOL) and transmission electron microscopy, respectively (TEM, JEOL-JSM-1400 PLUS) [50]. Elimination of genetic materials and total protein was assessed by gel electrophoresis. DNA was extracted using G-spin™ Total DNA Extraction Kit

(iNTRON, Co. Korea) according to the manufacturer's instructions. The isolated DNA was subjected to 1% agarose gel electrophoresis and visualized under a UV-transilluminator. The protein content of the cytoplasm and the envelope (cell wall and cell membrane) was estimated using the Bradford method [51] and BSA as a standard protein. All protein samples were subjected to 12% SDS-PAGE as reported [52]. The integrity of the LAGs capsules was assessed by light microscopy following staining with crystal violet/copper sulphate (Anthony's stain) consisting of crystal violet as primary stain and 20% copper sulphate solution as decolorizing solution and counter stain [53]. Finally, the LAGs surface negativity was examined using nigrosine staining. This was performed by mixing a small drop of nigrosine solution (10% w/v) with a small drop of bacterial or ghost suspension near the end of a glass slide and the mixture spread into a thin smear and examined under the oil immersion lens of a light microscope after air drying [54].

Preparation, purification, and characterization of prodigiosin. Prodigiosin (PG) was produced by *S. marcescens*, obtained from the Microbial Biotechnology Laboratory, Institute of Graduate Studies and Research, Alexandria University. The bacterial strain was identified biochemically at the Department of Microbiology, Faculty of Medicine, Alexandria University. PG was prepared, purified, and characterized as reported [41].

Prodigiosin-functionalized L. acidophilus **ghosts (PG-LAGs)**.

Preparation. Ghost pellets were incubated with 1 mL PG solution (6 mg/mL) in a methanol: acetic acid (1: 1) solvent system with gentle shaking at ambient temperature (≈ 28˚C) for 2 h. The PG-loaded ghosts (PG-LAGs) were separated by centrifugation at 24192 xg for 5 min, washed twice using 0.5% NaCl and stored at 4˚C suspended in 0.5% NaCl. The effect of solvent system composition (methanol: acetic acid ratio 1:0, 1:1, and 3:1), PG concentration (100–6000 μg/mL) and incubation time (0.5–5h) at the agitation rate 200 rpm on PG loading was examined. For the determination of drug payload, PG was extracted from LAGs by vigorous shaking with methanol for 10 min and assayed by UV-Vis spectrophotometry at λ_{max} 535 nm. The % loading efficiency was calculated as follows:

$$\mathrm{Loadingefficiency\%} = \frac{\mathrm{EntrappedPG(mg)}}{\mathrm{Ghostweight(g)}}$$

Verification of PG entrapment in LAGs. PG-LAGs were examined in comparison with blank LAGs by digital photography, light microscopy without staining and TEM.

Physical characterization. The size, polydispersity index (PDI) and zeta potential (ZP) of PG-LAGs in comparison with blank LAGs were measured by dynamic light scattering (DLS) using Zetasizer Nano ZS (Malvern Zeta Sizer, UK).

Release studies. The *in vitro* release of PG from PG-LAGs was studied at 37˚C by a dialysis method [43] using acetate buffer pH 5.5 and phosphate buffer saline (PBS) pH 7.4 with or without the addition of 5% 1 mL of PG-LAG suspension in 0.5% saline was

placed in a dialysis bag (VISKING® dialysis tubing MWCO 12,000–14,000) and shaken in 10 mL of the release medium at 60 rpm for 24 h protected from light. In addition, PG release was examined in simulated gastrointestinal fluids by immersing PG-LAGs in simulated gastric fluid (SGF, 10 mL pepsin / HCl, 320 mg/100 mL, pH 1.2) for 2 h followed by immersion in simulated intestinal fluid (SIF, 10 mL of pancreatin / PBS, 1 g/100 mL, pH 7.2) for 4 h. Samples of the release medium (2 mL) were withdrawn for analysis at different time intervals and replaced with 2 mL of fresh medium at 37°C. The concentration of PG released was determined by UV-Vis spectrophotometry at λ_{max} 535 nm.

Cytotoxicity studies. The cytotoxicity of PG-LAGs in comparison with blank LAGs, PG, and 5-fluorouracil (5-FU) was assessed at different concentrations using HCT116 colorectal cancer (CRC) cell line and normal human fibroblasts (American Type Culture Collection (ATCC, USA). The cells were cultured in DMEM supplemented with 10% FBS and 1% penicillin/streptomycin and maintained in an incubator with 5% carbon dioxide and humidified air at 37°C. Stock solutions of PG and 5-FU in DMSO and stock suspensions of live LA cells, blank LAGs and PG-LAGs were diluted in DMEM to reach the respective required concentrations. DMEM containing the equivalent amount of DMSO used in the other treatment groups (1%) was used as a control. Cell viability was assessed by MTT assay as reported earlier [55]. Briefly, cells were seeded in 96-well plates (4000 cells/well) and maintained overnight at 37°C. Media were replaced with 100 µl of test preparations including PG solution (0.25-10 µg/mL) and 5-FU solution (0.25-10 µg/mL) as well as suspensions of live LA cells (62.5-1500 µg/mL), LAGs (37.5-1500 µg/mL), and PG-LAGs (1:25 with PG concentration 0.25-10 µg/mL) and the cells incubated for 24 h. Media were then discarded, and the cells incubated with 20 µL MTT reagent (5 mg/mL) for 4 h. The resulting formazan crystals were dissolved in 150 µL of DMSO and the absorbance at 590 nm was recorded using a Bio-Rad microplate reader.

Cell viability, IC50 values and selectivity index (SI). The % viability of HTT-116 cells was determined in triplicate relative to the control wells. The median inhibitory concentrations (IC50) were determined using CompuSyn software (CompuSyn, Inc., version 1) according to the Chou-Talalay method [56]. The selectivity of PG-LAGs for HCT116 CRC cells in comparison with LAGs, PG, and 5-FU was assessed by calculating the selectivity index (SI) as follows [55]:

$$\mathrm{SI} = \frac{\mathrm{IC50innormalfibroblasts}}{\mathrm{IC50inCHT116CRCcellline}}$$

Combination index (CI) and dose reduction index (DRI). For the analysis of the combinatorial effects of PG and LAGs in the PG-LAGs combination on HCT116 CRC cell line, the type of interactive effect of PG and LAGs was examined by determining the Combination Index (CI) and Dose Reduction Index (DRI) using CompuSyn software [56].

Effect of test preparations on apoptosis-related biomarkers in HCT116 cell lysates. Cell lysates were obtained using RIPA (Radioimmunoprecipitation assay) lysis and extraction Buffer (Thermo Scientific, USA (#89900) containing 25 mM Tris-HCl pH 7.6, 150 mM NaCl, 1% NP-40 (nonyl

phenoxypolyethoxylethanol), 1% sodium deoxycholate, and 0.1% SDS. HCT116 cell pellets were mixed with 1 mL RIPA buffer (containing a protease inhibitor cocktail), shaken gently for 15 min on ice and centrifuged at 14000 ×g for 15 min to pellet the cell debris. The supernatants were separated and stored at -20 °C pending determination of the total amount of cellular protein extracted from the cells using the Bradford assay [57].

Caspase-3 activity. The level of active caspase-3 in cell lysates was determined using a colorimetric kit (# ab39401, Abcam) as reported [55]. A p-nitroaniline moiety released after hydrolysis of the peptide substrate (Ac-DEVD-pNA) by active caspase-3 in cell lysates was quantified using a calibration curve constructed from absorbance at 405 nm measured on a microtitre plate. Data are the mean ± SEM of three replica.

P53 and BCL 2 proteins. The levels of P53 and BCL 2 proteins per gram of total cellular protein in the cell lysate were determined using Human Immunoassay Elisa kits (ab171571- p53 Human SimpleStep ELISA® Kit) and (ab119506 - Bcl-2 Human ELISA® Kit) respectively according to the manufacturer's instructions. The p53 and Bcl-2 protein levels were normalized by cell viability for each treatment. Independent experiments with three replicates were performed for each protein and the mean abundances from each of the experiments were pooled for statistical analysis. Finally, the amount of P53 and BCL 2 per g of total cellular protein was determined.

Statistical analysis

Data were analyzed using Graph Pad Prism® version 6 software (GraphPad Software Inc., CA, USA). Multiple comparisons were analyzed by one-way analysis of variance (ANOVA) then post hoc Tukey's multiple comparison test. Data expressed as means ± SD are representative of three measurements. A value of $p < 0.05$ was indicative of significance.

Data availability

Data sets generated or analyzed during the study are included in the article

Declarations

Author contributions

L.E and A. H. conceptualized the research ideas. A.H, L.K., H.E and H.M. supervised the work. N.S., H.M., H.E. and M.H. contributed to methodology development. N.S., H.M. H.E. and M.H. contributed to experimental work and data analysis. N.S. prepared the original draft. N.S., H.E., H.M. and L.K. prepared the figures. L.K., H.E. and H.M. wrote and edited the final manuscript. All authors reviewed the manuscript.

Competing interests

The authors declare no competing interests.

Additional information

Correspondence and requests for materials should be addressed to A.H.

References

1. Cao, Z. & Liu, J. Bacteria and bacterial derivatives as drug carriers for cancer therapy. *J Control Release.* **326**, 396–407 https://doi.org/10.1016/j.jconrel.2020.07.009 (2020).
2. Harisa, G. I., Sherif, A. Y., Youssof, A. M. E., Alanazi, F. K. & Salem-Bekhit, M. M. Bacteriosomes as a Promising Tool in Biomedical Applications: Immunotherapy and Drug Delivery. *AAPS PharmSciTech.* **21**, 168 https://doi.org/10.1208/s12249-020-01716-x (2020).
3. Abdel-Razek, A. S., El-Naggar, M. E., Allam, A., Morsy, O. M. & Othman, S. I. Microbial natural products in drug discovery. *Processes.* **8**, 470 (2020).
4. Langemann, T. *et al.* The Bacterial Ghost platform system: production and applications. *Bioengineered bugs.* **1**, 326–336 https://doi.org/10.4161/bbug.1.5.12540 (2010).
5. Rabea, S. *et al.* A novel protocol for bacterial ghosts' preparation using tween 80. *Saudi Pharm J.* **26**, 232–237 https://doi.org/10.1016/j.jsps.2017.12.006 (2018).
6. Vinod, N. *et al.* Generation of a novel Staphylococcus aureus ghost vaccine and examination of its immunogenicity against virulent challenge in rats. *Infection and immunity.* **83**, 2957–2965 (2015).
7. Huter, V. *et al.* Bacterial ghosts as drug carrier and targeting vehicles. *Journal of controlled release.* **61**, 51–63 (1999).
8. Langemann, T. *et al.* The Bacterial Ghost platform system: production and applications. *Bioengineered bugs.* **1**, 326–336 https://doi.org/10.4161/bbug.1.5.12540 (2010).
9. Batah, A. M. & Ahmad, T. A. The development of ghost vaccines trials. *Expert review of vaccines.* **19**, 549–562 https://doi.org/10.1080/14760584.2020.1777862 (2020).
10. Groza, D. *et al.* Bacterial ghosts as adjuvant to oxaliplatin chemotherapy in colorectal carcinomatosis. *Oncoimmunology.* **7**, e1424676–e1424676 https://doi.org/10.1080/2162402X.2018.1424676 (2018).
11. Alanazi, F. K. *et al.* Vision of bacterial ghosts as drug carriers mandates accepting the effect of cell membrane on drug loading. *Drug Dev Ind Pharm.* **46**, 1716–1725 https://doi.org/10.1080/03639045.2020.1820039 (2020).
12. Rabea, S. *et al.* Salmonella-innovative targeting carrier: Loading with doxorubicin for cancer treatment. *Saudi Pharm J.* **28**, 1253–1262 https://doi.org/10.1016/j.jsps.2020.08.016 (2020).
13. Youssof, A. M. E., Alanazi, F. K., Salem-Bekhit, M. M., Shakeel, F. & Haq, N. Bacterial Ghosts Carrying 5-Fluorouracil: A Novel Biological Carrier for Targeting Colorectal Cancer. *AAPS PharmSciTech.* **20**, 48 https://doi.org/10.1208/s12249-018-1249-z (2019).

14. Xie, S. *et al.* Bacterial ghosts for targeting delivery and subsequent responsive release of ciprofloxacin to destruct intracellular bacteria. *Chem. Eng. J.* **399**, 125700 (2020).
15. Mohammadi, E. & Golchin, M. High protection of mice against Brucella abortus by oral immunization with recombinant probiotic Lactobacillus casei vector vaccine, expressing the outer membrane protein OMP19 of Brucella species. *Comparative immunology, microbiology and infectious diseases.* **70**, 101470 (2020).
16. Śliżewska, K., Markowiak-Kopeć, P. & Śliżewska, W. The Role of Probiotics in Cancer Prevention. *Cancers.* **13**, 20 (2021).
17. El-Deeb, N. M., Yassin, A. M., Al-Madboly, L. A. & El-Hawiet, A. A novel purified Lactobacillus acidophilus 20079 exopolysaccharide, LA-EPS-20079, molecularly regulates both apoptotic and NF-kappaB inflammatory pathways in human colon cancer. *Microb Cell Fact.* **17**, 29 https://doi.org/10.1186/s12934-018-0877-z (2018).
18. Nishiyama, K., Sugiyama, M. & Mukai, T. Adhesion Properties of Lactic Acid Bacteria on Intestinal Mucin. *Microorganisms.* **4**, https://doi.org/10.3390/microorganisms4030034 (2016).
19. Azad, M., Kalam, A., Sarker, M. & Wan, D. Immunomodulatory effects of probiotics on cytokine profiles. BioMed research international 2018 (2018).
20. Rabea, S. *et al.* Salmonella-innovative targeting carrier: Loading with doxorubicin for cancer treatment. *Saudi Pharm J.* **28**, 1253–1262 https://doi.org/10.1016/j.jsps.2020.08.016 (2020).
21. Lapenda, J. C. L., Alves, V. P., Adam, M. L., Rodrigues, M. D. & Nascimento, S. C. Cytotoxic Effect of Prodigiosin, Natural Red Pigment, Isolated from Serratia marcescens UFPEDA 398. *Indian J Microbiol.* **60**, 182–195 https://doi.org/10.1007/s12088-020-00859-6 (2020).
22. Ho, T. F. *et al.* Prodigiosin down-regulates survivin to facilitate paclitaxel sensitization in human breast carcinoma cell lines. *Toxicology and applied pharmacology.* **235**, 253–260 (2009).
23. Hassankhani, R., Sam, M. R., Esmaeilou, M. & Ahangar, P. Prodigiosin isolated from cell wall of Serratia marcescens alters expression of apoptosis-related genes and increases apoptosis in colorectal cancer cells. *Med Oncol.* **32**, 366 https://doi.org/10.1007/s12032-014-0366-0 (2015).
24. Sam, S., Sam, M. R., Esmaeillou, M. & Safaralizadeh, R. Effective Targeting Survivin, Caspase-3 and MicroRNA-16-1 Expression by Methyl-3-pentyl-6-methoxyprodigiosene Triggers Apoptosis in Colorectal Cancer Stem-Like Cells. *Pathol Oncol Res.* **22**, 715–723 (2016).
25. Prabhu, V. V. *et al.* Small-Molecule Prodigiosin Restores p53 Tumor Suppressor Activity in Chemoresistant Colorectal Cancer Stem Cells via c-Jun-Mediated DeltaNp73 Inhibition and p73 Activation. *Cancer Res.* **76**, 1989–1999 https://doi.org/10.1158/0008-5472.CAN-14-2430 (2016).
26. Zhao, C. *et al.* Prodigiosin impairs autophagosome-lysosome fusion that sensitizes colorectal cancer cells to 5-fluorouracil-induced cell death. *Cancer Lett.* **481**, 15–23 https://doi.org/10.1016/j.canlet.2020.03.010 (2020).
27. Amara, A. A., Salem-Bekhit, M. M. & Alanazi, F. K. Preparation of bacterial ghosts for E. coli JM109 using sponge-like reduced protocol. *Asian J Biol Sci.* **6**, 363–369 (2013).

28. Sridharan, G. & Shankar, A. A. Toluidine blue: A review of its chemistry and clinical utility. *J Oral Maxillofac Pathol.* **16**, 251–255 https://doi.org/10.4103/0973-029X.99081 (2012).
29. Mortimer, M., Petersen, E. J., Buchholz, B. A. & Holden, P. A. Separation of Bacteria, Protozoa and Carbon Nanotubes by Density Gradient Centrifugation. *Nanomaterials (Basel).* **6**, https://doi.org/10.3390/nano6100181 (2016).
30. Nwodo, U. U., Green, E. & Okoh, A. I. Bacterial exopolysaccharides: functionality and prospects. *Int J Mol Sci.* **13**, 14002–14015 https://doi.org/10.3390/ijms131114002 (2012).
31. Halder, S. *et al.* Alteration of Zeta potential and membrane permeability in bacteria: a study with cationic agents. *SpringerPlus.* **4**, 1–14 (2015).
32. Schar-Zammaretti, P. & Ubbink, J. The cell wall of lactic acid bacteria: surface constituents and macromolecular conformations. *Biophys J.* **85**, 4076–4092 https://doi.org/10.1016/S0006-3495(03)74820-6 (2003).
33. Velez, M. P., De Keersmaecker, S. C. & Vanderleyden, J. Adherence factors of Lactobacillus in the human gastrointestinal tract. *FEMS Microbiol Lett.* **276**, 140–148 https://doi.org/10.1111/j.1574-6968.2007.00908.x (2007).
34. Guryanov, I. *et al.* Selective Cytotoxic Activity of Prodigiosin@halloysite Nanoformulation. *Front Bioeng Biotechnol.* **8**, 424 https://doi.org/10.3389/fbioe.2020.00424 (2020).
35. Suryawanshi, R. K., Patil, C. D., Koli, S. H., Hallsworth, J. E. & Patil, S. V. Antimicrobial activity of prodigiosin is attributable to plasma-membrane damage. *Natural product research.* **31**, 572–577 (2017).
36. Obayemi, J. D. *et al.* PLGA-based microparticles loaded with bacterial-synthesized prodigiosin for anticancer drug release: Effects of particle size on drug release kinetics and cell viability. *Materials science & engineering. C, Materials for biological applications.* **66**, 51–65 https://doi.org/10.1016/j.msec.2016.04.071 (2016).
37. Gabba, M. *et al.* Weak Acid Permeation in Synthetic Lipid Vesicles and Across the Yeast Plasma Membrane. *Biophys J.* **118**, 422–434 https://doi.org/10.1016/j.bpj.2019.11.3384 (2020).
38. Ingolfsson, H. I. & Andersen, O. S. Alcohol's effects on lipid bilayer properties. *Biophys J.* **101**, 847–855 https://doi.org/10.1016/j.bpj.2011.07.013 (2011).
39. Gjadhar, S. & Mellem, J. J. Isolation and characterization of a microbial pigment obtained from Serratia marcescens as a natural food colourant. *The Annals of the University Dunarea de Jos of Galati. Fascicle VI-Food Technology.* **43**, 137–154 (2019).
40. Gong, J. *et al.* Bio-Preparation and Regulation of Pyrrole Structure Nano-Pigment Based on Biomimetic Membrane. *Nanomaterials (Basel).* **9**, https://doi.org/10.3390/nano9010114 (2019).
41. Dozie-Nwachukwu, S. O. *et al.* Extraction and encapsulation of prodigiosin in chitosan microspheres for targeted drug delivery. *Materials science & engineering. C, Materials for biological applications.* **71**, 268–278 https://doi.org/10.1016/j.msec.2016.09.078 (2017).
42. Koller, V. J. *et al.* Modulation of bacterial ghosts–induced nitric oxide production in macrophages by *al.* **280**, 1214–1225 (2013).

43. Paukner, S., Kohl, G. & Lubitz, W. Bacterial ghosts as novel advanced drug delivery systems: antiproliferative activity of loaded doxorubicin in human Caco-2 cells. *J Control Release.* **94**, 63–74 https://doi.org/10.1016/j.jconrel.2003.09.010 (2004).
44. Gruenberg, J. & van der Goot, F. G. Mechanisms of pathogen entry through the endosomal compartments. *Nature Reviews Molecular Cell Biology.* **7**, 495–504 https://doi.org/10.1038/nrm1959 (2006).
45. Haslberger, A. G. *et al.* Activation, stimulation and uptake of bacterial ghosts in antigen presenting cells. *Journal of biotechnology.* **83**, 57–66 https://doi.org/10.1016/s0168-1656(00)00298-4 (2000).
46. Stein, E. *et al.* In vitro and in vivo uptake study of Escherichia coli Nissle 1917 bacterial ghosts: cell-based delivery system to target ocular surface diseases. *Invest Ophthalmol Vis Sci.* **54**, 6326–6333 https://doi.org/10.1167/iovs.13-12044 (2013).
47. Yeung, T. M., Gandhi, S. C., Wilding, J. L., Muschel, R. & Bodmer, W. F. Cancer stem cells from colorectal cancer-derived cell lines. Proceedings of the National Academy of Sciences 107, 3722–3727(2010).
48. Cho, Y. H. *et al.* 5-FU promotes stemness of colorectal cancer via p53-mediated WNT/beta-catenin pathway activation. *Nat Commun.* **11**, 5321 https://doi.org/10.1038/s41467-020-19173-2 (2020).
49. Scherr, A. L. *et al.* Bcl-xL is an oncogenic driver in colorectal cancer. *Cell Death Dis.* **7**, e2342–e2342 https://doi.org/10.1038/cddis.2016.233 (2016).
50. Tahmasebi, P., Javadpour, F. & Sahimi, M. Three-dimensional stochastic characterization of shale SEM images. *Transport in Porous Media.* **110**, 521–531 (2015).
51. Bradford, M. M. A rapid and sensitive method for the quantitation of microgram quantities of protein utilizing the principle of protein-dye binding. *Analytical biochemistry.* **72**, 248–254 (1976).
52. Laemmli, U. K. Cleavage of structural proteins during the assembly of the head of bacteriophage T4. nature 227, 680–685(1970).
53. Oleksy, M. & Klewicka, E. Capsular Polysaccharides of Lactobacillus spp.: Theoretical and Practical Aspects of Simple Visualization Methods. *Probiotics and antimicrobial proteins.* **9**, 425–434 (2017).
54. Bisen, P. Microbial staining. *Microbes in Practice. IK International, New Delhi, India*,139–155(2004).
55. Helmy, M. W., Ghoneim, A. I., Katary, M. A. & Elmahdy, R. K. The synergistic anti-proliferative effect of the combination of diosmin and BEZ-235 (dactolisib) on the HCT-116 colorectal cancer cell line occurs through inhibition of the PI3K/Akt/mTOR/NF-κB axis. *Mol Biol Rep.* **47**, 2217–2230 https://doi.org/10.1007/s11033-020-05327-4 (2020).
56. Chou, T. C. Drug combination studies and their synergy quantification using the Chou-Talalay method. *Cancer Res.* **70**, 440–446 https://doi.org/10.1158/0008-5472.Can-09-1947 (2010).
57. Bradford, M. M. A rapid and sensitive method for the quantitation of microgram quantities of protein utilizing the principle of protein-dye binding. *Anal. Biochem.* **72**, 248–254 https://doi.org/10.1016/0003-2697(76)90527-3 (1976).

Figures

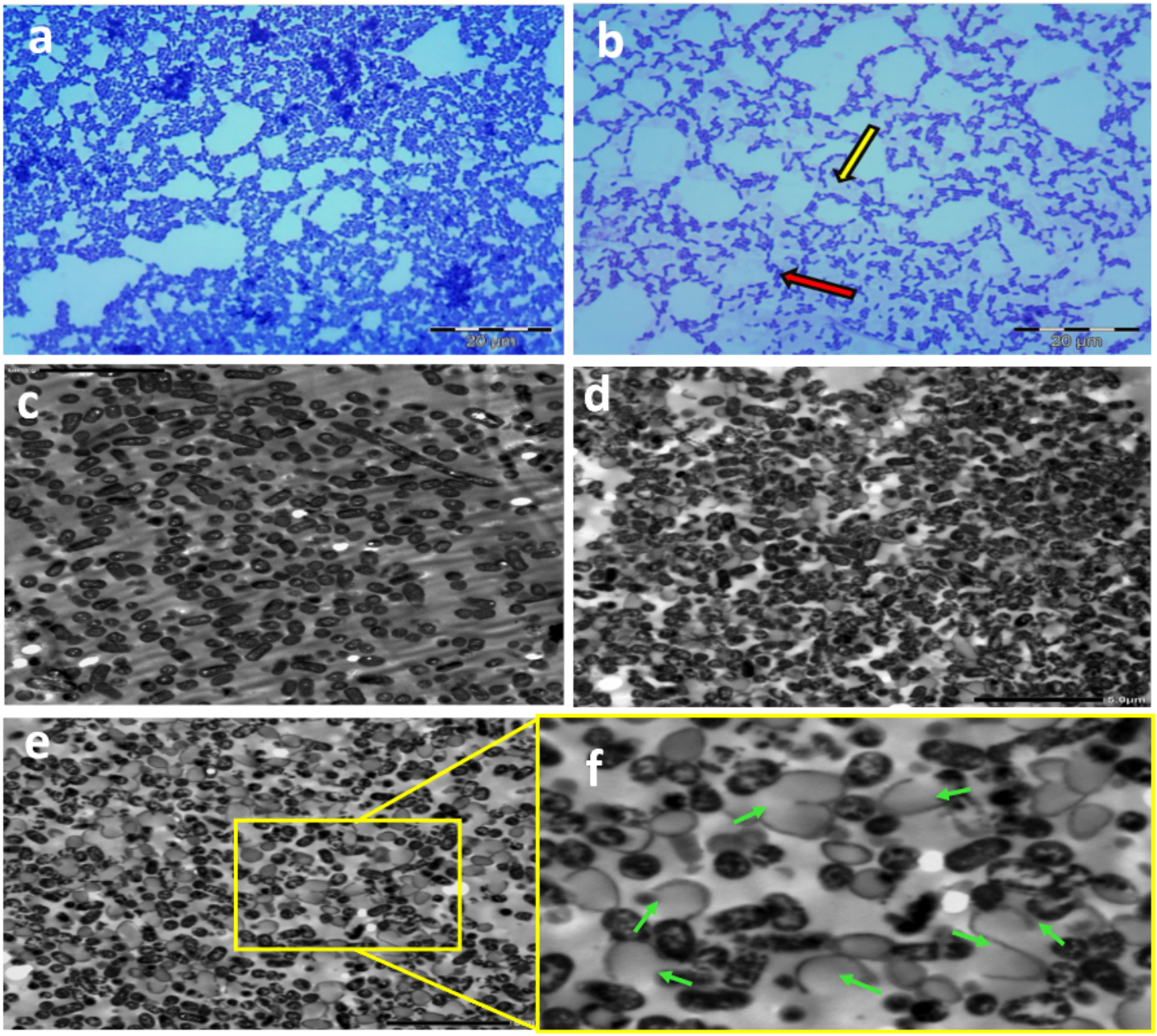

Figure 1

Microscopic examination of Live L. acidophilus (LA) cells and the bacterial mass consisting of LA cells (live and dead un-evacuated) and L. acidophilus ghosts (LAGs). a. and b. Light microscopic images at 100x following toluidine blue staining of a. Live LA cells and b. bacterial mass. The red and yellow arrows point to stained un-evacuated LA cells and unstained LAGs, respectively. c-f. TEM of c. Live LA cells, d and e. Bacterial mass obtained after chemical treatment under shaking and static conditions, respectively (1500x) and f. Enlarged section of e showing deteriorated LAG cell wall (green arrows).

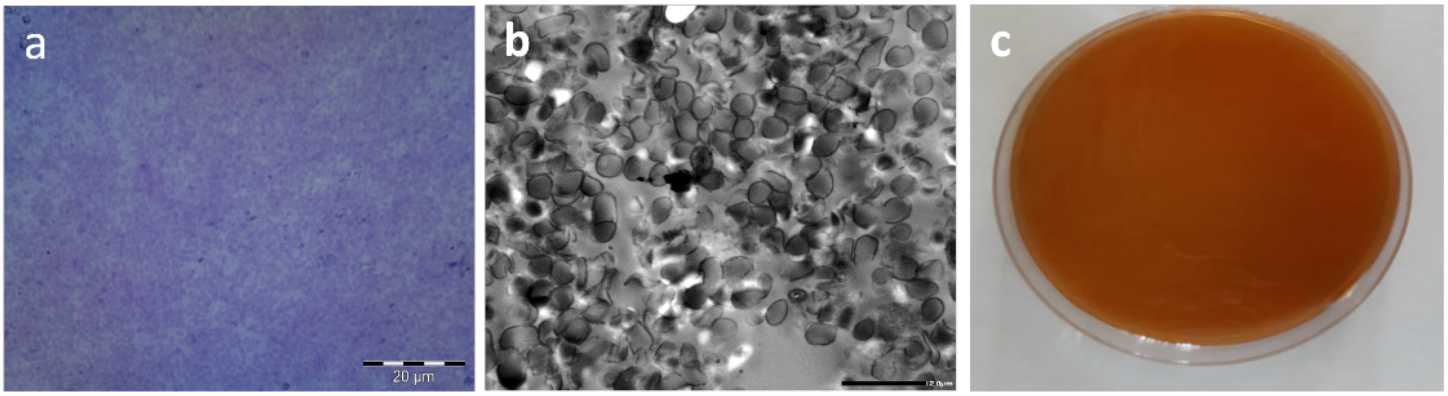

Figure 2

Efficiency of L. acidophilus ghost purification. a. Light microscopic image following toluidine staining at 100x. b. TEM at 3000x and c. MRS plate inoculated with LAGs for 48 h at 37°C.

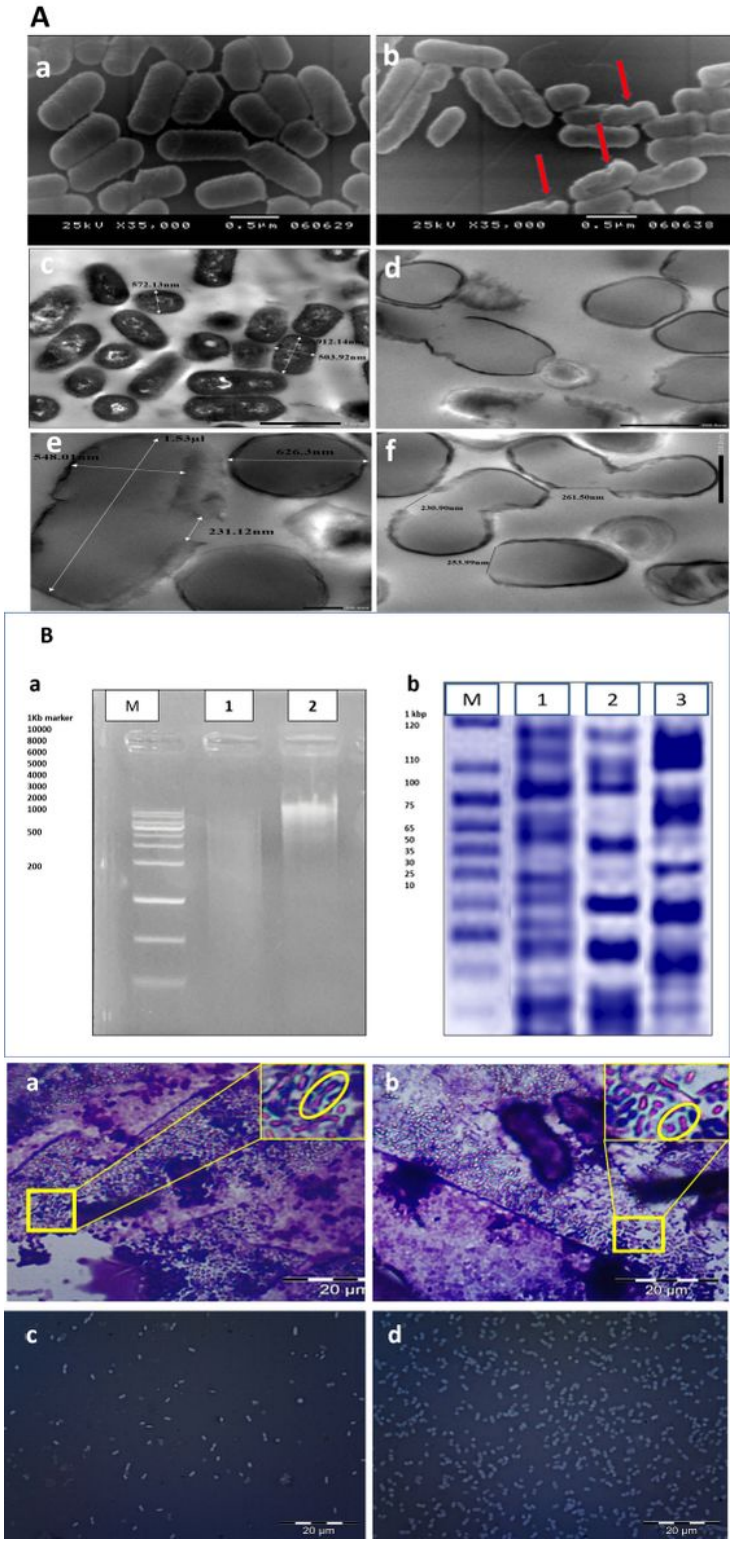

Figure 3

A. Electron microscopic characterization of L. acidophilus ghosts (LAGs) in comparison with live LA cells. Scanning electron micrographs at 35000x for a. live L. acidophilus cells and b. LAGs. Red arrows point to the pores from which cytoplasm and genetic materials were expelled. Transmission electron micrographs for c. Live LA cells at 8000x and d. LAGs at 15000x showing expulsion of cytoplasmic content, e. LAGs at 0x showing pore size. B. Detection of DNA and

proteins in live L. acidophilus (LA) and their ghosts (LAGs). a. DNA profile on agarose gel under UV transilluminator showing: M. 1 kbp marker, lane 1: DNA isolated from purified LAGs and lane 2: DNA isolated from live LA cells before chemical treatment. b. SDS-PAGE stained with Coomassie brilliant blue R250 for proteins of live LA cells, LAGs, and the supernatant after chemical treatment. M. Molecular weight marker, lane 1: LA cell proteins, Lane 2: LAG proteins and Lane 3: Intracellular proteins in the supernatant after chemical treatment. C. Light microscopic examination of the integrity and surface negativity of L. acidophilus ghosts (LAGs) in comparison with live LA cells at 100x magnification. Crystal violet/copper sulfate staining of a. Live LA cells and b. LAGs. The insets in Figures a and b show enlarged sections (yellow oval shape) highlighting live LA cells and LAGs respectively with intact capsule appearing as faint blue halos around the purple cell. Nigrosine staining revealed c. live LA cells and d. LAGs as bright halos on the dark background.

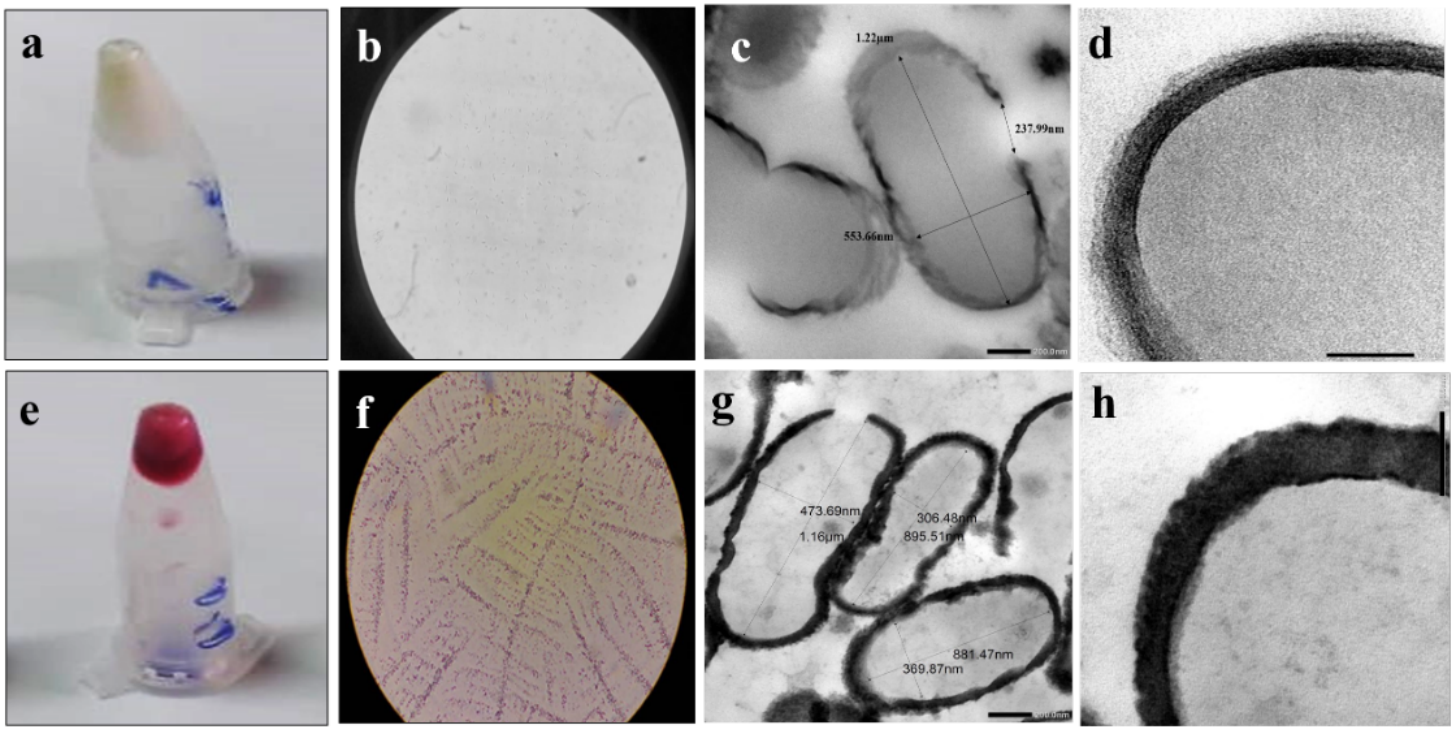

Figure 4

Images of blank L. acidophilus ghosts (LAGs, a-d) and prodigiosin-loaded LAGs (PG-LAGs, e-h). Digital photos of LAG and PG-LAG pellets in inverted Eppendorf tubes (a and e respectively). Images of LAGs and PG-LAGs under the oil immersion lens of the light microscope without staining (b and f respectively). Transmission electron micrographs for LAGs and PG-LAGs at 20000x (c and g respectively) and at 80000x (d and h respectively).

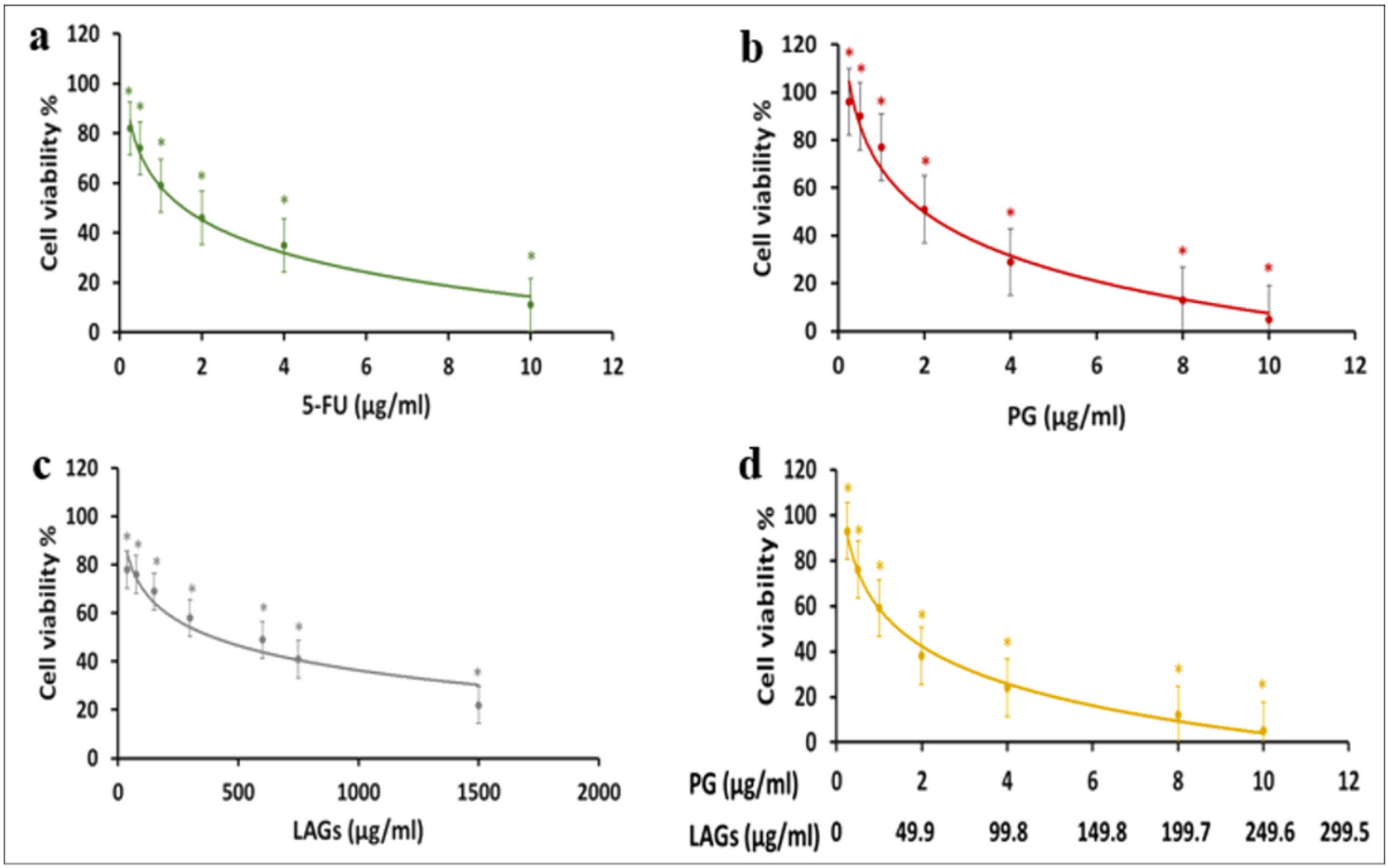

Figure 5

HCT116 viability curves. The % viability of HCT116 cells determined using the MTT assay upon treatment with a. 5-fluorouracil (5-FU), b. prodigiosin (PG), c. L. acidophilus ghost (LAGs) and d. PG loaded ghosts (PG-LAGs) at increasing concentrations for 24 h. Data points represent the mean ± SEM (n=3). *p < 0.05 indicates a significant difference vs the corresponding control group.

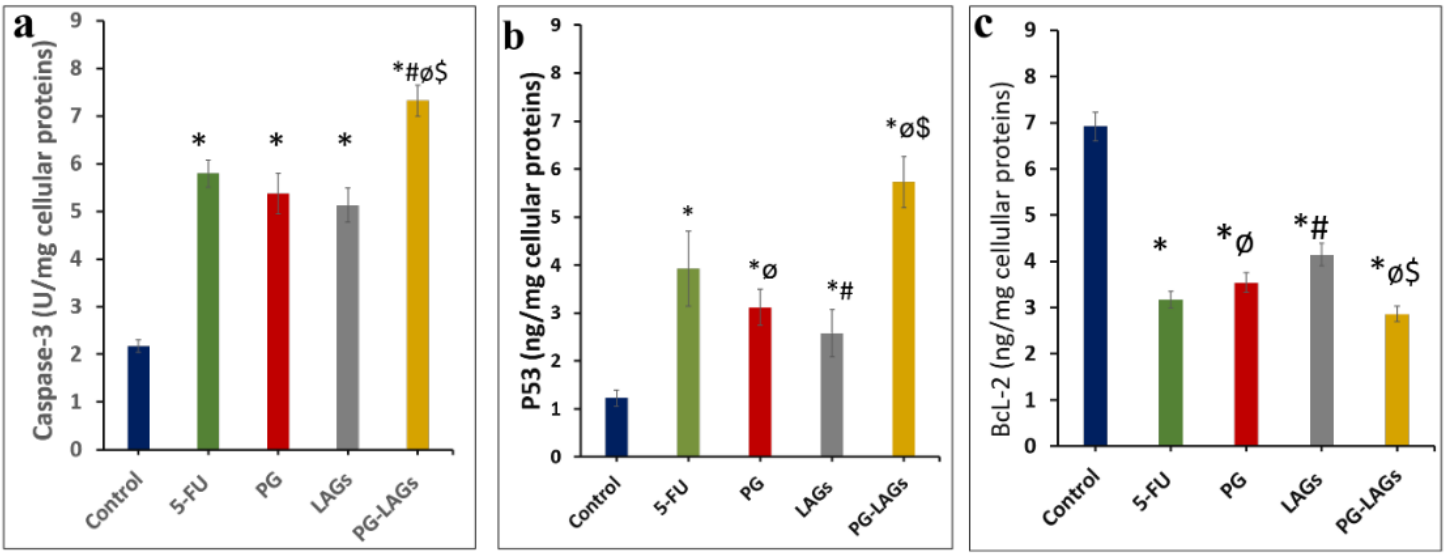

Figure 6

Effect of test preparations on apoptosis-related biomarkers. Effect of 5-FU (1.48 µg/ml), PG (2.03 µg/ml), LAGs (393.44 µg/ml) and PG-LAGs (46.47 µg/ml total dose) in comparison with control on the level of a. Caspase 3 determined colorimetrically and b. P53 and c. BCL 2, both determined by ELISA assay. Protein levels were estimated per mg of HCT116 cellular protein. Data points represent the mean ± SEM (n=3) *, #, ø and $ ($p<0.05$) indicate a significant difference vs the corresponding control, 5-FU, LAGs, and PG, respectively.

Supplementary Files

This is a list of supplementary files associated with this preprint. Click to download.

- Supplementaryfile.pdf